R. & M. No. 3197
(21,333)
A.R.C. Technical Report

R. & M. No. 3197

MINISTRY OF AVIATION

AERONAUTICAL RESEARCH COUNCIL
REPORTS AND MEMORANDA

# Leading-Edge Buckling due to Aerodynamic Heating

By E. H. MANSFIELD, Sc.D.

LONDON: HER MAJESTY'S STATIONERY OFFICE
1960
EIGHT SHILLINGS NET

# Leading-Edge Buckling due to Aerodynamic Heating

By E. H. Mansfield, Sc.D.

Communicated by Deputy Controller Aircraft (Research & Development)
Ministry of Supply

*Reports and Memoranda No.* 3197*

*May*, 1959

*Summary.*—A simple formula is derived for determining the onset of leading-edge buckling due to aerodynamic heating of wings which are either solid or thin-walled with a shear-resistant filling. The post-buckling behaviour is also investigated.

1. *Introduction.*—Aerodynamic heating of a thin wing causes spanwise temperature stresses which are compressive at the leading and trailing edges and tensile at the mid chord[1]. These stresses reduce the torsional and flexural rigidities of the wing[2,3,4]. However, if the compressive stresses are sufficiently localised in the region of the leading edge, buckling will occur there at a lower intensity of stress than that required for complete loss of torsional or flexural rigidity.

The present paper considers leading-edge buckling in wings which are either solid or thin-walled with a continuous shear-resistant filling. It is shown that buckling commences when the spanwise stress at the leading edge reaches a value which depends on the shear modulus of the material and the wing geometry at the leading edge; furthermore, the spanwise wavelength is initially very small. The post-buckling behaviour is also investigated and it is shown that with increasing stress the wavelength and the magnitude of the buckles increase.

2. *Method of Solution.*—The assumptions made and their implications are outlined in Section 2.1.

Chordwise variations of temperature in the wing cause spanwise middle-surface forces which are self-equilibrating. In Section 2.2 the conditions of self-equilibration are shown to be satisfied if the middle-surface forces are derived from a type of force function. In Section 2.3 the conditions for buckling in terms of such a force function are outlined and it is noted that a particular force function (one, in fact, which is simply related to the variable wing rigidity) will have special properties. These special properties are discussed in Section 3.

2.1. *Assumptions.*—The following assumptions are made:

(i) The wing is of infinite aspect ratio

(ii) The temperature and wing structure do not vary along the span

* R.A.E. Report Structures 250, received 21st October, 1959.

(iii) The wing acts as a plate (of variable rigidity)

(iv) The shear-resistant filling in the thin-walled wing has no direct stiffness in the plane of the wing

(v) The wing section has sharp leading and trailing edges

(vi) The effect of externally applied forces or moments is not considered

(vii) The elastic constants and the coefficient of thermal expansion do not vary with temperature

(viii) Temperatures due to aerodynamic heating are symmetrical about the mid-plane of the wing.

The results obtained in this paper may be applied, despite assumptions (i) and (ii), to wings of low aspect ratio and high taper or sweep because of the essentially localised character of leading-edge buckling. The analysis cannot be applied to a hollow built-up wing for which assumption (iii) is untenable. Assumption (iv) is standard practice; appropriate allowances could be made if necessary. As for assumption (v), leading-edge buckling will not occur unless the leading edge is, for practical purposes, sharp. Assumption (vi) is unlikely to have any significant effect on leading-edge buckling, although a large applied bending moment or torque would tend to stabilise the leading edge. Assumption (vii) is not essential to the analysis and account can readily be taken of temperature dependent properties. Assumption (viii) implies that the heat transfer through the upper and lower surfaces of the wing is the same. The buckling behaviour of the wing depends only on the resultant of the stresses through the wing thickness and hence only on the average temperature through the wing thickness.

2.2. *Spanwise Equilibrium of Middle-Surface Forces.*—The spanwise middle-surface forces/unit length, $N_y$ must satisfy the conditions of self-equilibration

$$\left.\begin{aligned} \int_{-c/2}^{c/2} N_y \, dx &= 0 \\ \int_{-c/2}^{c/2} x N_y \, dx &= 0 \end{aligned}\right\} \qquad \ldots \quad \ldots \quad \ldots \quad \ldots \quad (1)$$

These conditions are automatically satisfied by introducing a force function $\Phi$ from which the forces/unit length are obtained by double differentiation:

$$N_y = \frac{d^2\Phi}{dx^2}, \qquad \ldots \quad \ldots \quad \ldots \quad \ldots \quad \ldots \quad (2)$$

provided the force function satisfies the following boundary conditions:

$$\left(\Phi = \frac{d\Phi}{dx} = 0\right)_{x = \pm c/2}. \qquad \ldots \quad \ldots \quad \ldots \quad \ldots \quad (3)$$

It follows from these definitions of $\Phi$ that for any given distribution of forces $N_y$ there is one corresponding force function $\Phi$, and *vice versa*. The advantage of introducing this force function will appear in Section 3, where attention is given to a particular force function which has the unique property that under the action of the associated forces, buckling is equally likely to occur in any one of an infinite variety of modes, including torsion, flexure and leading-edge waving.

2.3. *General Conditions for Buckling.*—In determining the magnitude of the force function which will cause buckling it is convenient to write

$$\Phi = \gamma \Phi_0, \quad \ldots \quad \ldots \quad \ldots \quad \ldots \quad \ldots \quad \ldots \quad (4)$$

where $\gamma$ is a constant of proportionality while the magnitude of $\Phi_0$ is fixed. A proportional increase in the stresses throughout the wing is then represented by an increase in $\gamma$.

At the onset of buckling the release of middle-surface strain energy, which can be regarded as the work done by the forces $N_y$, is equal to the strain energy of bending. Thus, equating these energies and regarding compressive $N_y$ as positive[5], gives

$$\frac{1}{2}\int\int N_y \left(\frac{\partial w}{\partial y}\right)^2 dx\, dy = \frac{1}{2}\int\int D\left[(\nabla^2 w)^2 + 2(1-\nu)\left\{\left(\frac{\partial^2 w}{\partial x\, \partial y}\right)^2 - \frac{\partial^2 w}{\partial x^2}\frac{\partial^2 w}{\partial y^2}\right\}\right] dx\, dy, \quad \ldots \quad (5)$$

whence, from equations (3) and (4)

$$\gamma = \frac{\int\int D\left[(\nabla^2 w)^2 + 2(1-\nu)\left\{\left(\frac{\partial^2 w}{\partial x\, \partial y}\right)^2 - \frac{\partial^2 w}{\partial x^2}\frac{\partial^2 w}{\partial y^2}\right\}\right] dx\, dy}{\int\int \frac{d^2\Phi_0}{dx^2}\left(\frac{\partial w}{\partial y}\right)^2 dx\, dy} \quad \ldots \quad \ldots \quad (6)$$

and the magnitude of the forces at buckling may be found by determining the minimum value of $\gamma$. There will, in fact, be two 'minimum' values of practical interest corresponding to positive and negative $\gamma$.

It is shown in Appendix 1 by integrating by parts and using conditions (2) that the denominator in equation (6) may be transformed so that equation (6) may be written in an alternative form:

$$\gamma = \frac{\int\int D\left[(\nabla^2 w)^2 + 2(1-\nu)\left\{\left(\frac{\partial^2 w}{\partial x\, \partial y}\right)^2 - \frac{\partial^2 w}{\partial x^2}\frac{\partial^2 w}{\partial y^2}\right\}\right] dx\, dy}{2\int\int \Phi_0\left\{\left(\frac{\partial^2 w}{\partial x\, \partial y}\right)^2 - \frac{\partial^2 w}{\partial x^2}\frac{\partial^2 w}{\partial y^2}\right\}\right] dx\, dy} \quad \ldots \quad \ldots \quad (7)$$

So far, the analysis has been confined to a general formulation of the problem, and it is clear that an exact minimisation of $\gamma$ for a given variation of $D$ and a given force function $\Phi_0$ will not generally be possible. However, a comparison of the numerator and denominator in equation (7) suggests that the particular force function for which

$$\Phi_0 = D \quad \ldots \quad \ldots \quad \ldots \quad \ldots \quad \ldots \quad \ldots \quad (8)$$

may lend itself to an exact analysis. This particular force function, which is uniquely determined for any given wing section, satisfies the boundary conditions (2), by virtue of assumption (v), so that the corresponding forces $N_y$ are self-equilibrating.

A simple, yet rigorous, buckling analysis for this force function is given in Section 3. It is shown there that this force function has the unique and remarkable property that, under the action of the associated forces $N_y$, buckling can occur simultaneously in any combination of an infinite variety of modes including torsion, flexure and leading-edge waving. It is shown in Section 4 that this property of 'modal indeterminancy' may be used to determine the onset of leading-edge buckling in a wing with a different distribution of forces $N_y$.

3. *Buckling Characteristics of the Force Function* $\Phi = \gamma D$.—Substituting equations (7) and (8) in (6) gives

$$\gamma = 1 - \nu + \frac{\iint D\,(\nabla^2 w)^2\,dx\,dy}{2\iint D\left\{\left(\frac{\partial^2 w}{\partial x\,\partial y}\right)^2 - \frac{\partial^2 w}{\partial x^2}\,\frac{\partial^2 w}{\partial y^2}\right\}dx\,dy}. \qquad \ldots \quad \ldots \quad (9)$$

At this stage it is convenient to introduce the principal curvatures $\varkappa_1$, $\varkappa_2$ at any point in the plate for we have

$$\left.\begin{aligned} \varkappa_1 + \varkappa_2 &\equiv \nabla^2 w \\ \varkappa_1\,\varkappa_2 &\equiv \frac{\partial^2 w}{\partial x^2}\,\frac{\partial^2 w}{\partial y^2} - \left(\frac{\partial^2 w}{\partial x\,\partial y}\right)^2 \end{aligned}\right\} \qquad \ldots \quad \ldots \quad \ldots \quad (10)$$

and equation (9) then becomes

$$\gamma = 1 - \nu - \frac{\iint D(\varkappa_1 + \varkappa_2)^2\,dx\,dy}{2\iint D\varkappa_1\varkappa_2\,dx\,dy}. \qquad \ldots \quad \ldots \quad \ldots \quad (11)$$

The numerator in the fraction on the right-hand side of equation (11) is essentially positive and the sign of the denominator therefore determines the sign of $\gamma$. If the denominator is negative the minimum (positive) value for $\gamma$ occurs when

$$\left.\begin{aligned} \varkappa_1 + \varkappa_2 &= 0, \\ \text{i.e.,} \qquad \nabla^2 w &= 0 \end{aligned}\right\} \qquad \ldots \quad \ldots \quad \ldots \quad (12)$$

and is given by

$$\left.\begin{aligned} \gamma^{(+)} &= 1 - \nu \\ \text{so that} \qquad \Phi^{(+)} &= (1 - \nu)D \end{aligned}\right\} \qquad \ldots \quad \ldots \quad \ldots \quad (13)$$

Equation (12) confirms the assumption of a negative denominator. The case when the denominator is positive and $\gamma$ negative is considered in Appendix II.

4.1. *Buckling Modes Appropriate to* $\Phi^{(+)}$.—There are an infinite variety of buckling modes appropriate to equations (12) and (13) so that the actual mode shape is indeterminate. However, a typical mode (representing leading-edge or trailing-edge buckling) is given by

$$w \propto \left(\frac{\sin}{\cos}\right)(y/\lambda)\exp(\mp x/\lambda), \qquad \ldots \quad \ldots \quad \ldots \quad \ldots \quad (14)$$

where $\lambda$ is an arbitrary wavelength parameter; the smaller the value the more localised the buckling mode. As $\lambda$ tends to infinity all semblance of a localised character in the mode disappears and the mode tends to

$$w \propto xy \qquad \ldots \quad \ldots \quad \ldots \quad \ldots \quad \ldots \quad \ldots \quad \ldots \quad (15)$$

which represents torsional buckling, or

$$w \propto x^2 - y^2 \qquad \ldots \ldots \ldots \ldots \ldots \quad (16)$$

which represents flexural buckling. These modes are illustrated in Fig. 2.

In Section 4 it is shown that this property of 'modal indeterminancy' may be used to determine the onset of leading-edge buckling due to a different stress distribution. However, it is first necessary to consider in greater detail particular distributions of stresses appropriate to $\Phi^{(+)}$.

3.2. *Stress Distributions Appropriate to* $\Phi^{(+)}$.—To fix ideas, let us determine the stress distributions corresponding to the force function $\Phi^{(+)}$ for a number of representative wing sections. For an arbitrary chordwise variation of wing thickness $t$ the stress $\sigma_y^{(+)}$ can be expressed simply in terms of $t$ and its derivatives.

For a solid wing

$$\begin{aligned}\sigma_y^{(+)} &= N_y^{(+)}/t \\ &= \left(\frac{1-\nu}{t}\right)\frac{d^2}{dx^2}\left\{\frac{Et^3}{12(1-\nu^2)}\right\} \\ &= G\left\{\left(\frac{dt}{dx}\right)^2 + \frac{1}{2}t\frac{d^2t}{dx^2}\right\}. \qquad \ldots \ldots \ldots \quad (17)\end{aligned}$$

For a thin-walled wing

$$\begin{aligned}\sigma_y^{(+)} &= N_y^{(+)}/2h \\ &= \left(\frac{1-\nu}{2h}\right)\frac{d^2}{dx^2}\left\{\frac{Eht^2}{2(1-\nu^2)}\right\} \\ &= G\left\{\left(\frac{dt}{dx}\right)^2 + t\frac{d^2t}{dx^2}\right\}. \qquad \ldots \ldots \ldots \quad (18)\end{aligned}$$

3.2.1. *Chordwise Variation of* $\sigma_y^{(+)}$ *for some Typical Wing Sections.*—The chordwise variations of $\sigma_y^{(+)}$ for a number of typical wing sections have been determined from equations (17) and (18) and are plotted in Figs. 3 and 4 for solid and thin-walled wings respectively. The sections, which are all symmetrical ones, include a diamond section, a lenticular parabolic section and a lenticular sine section. The broken lines in Figs. 3 and 4 are typical of the chordwise variations of $\sigma_y$ due to aerodynamic heating.

3.3. *Leading-Edge Buckling vs. Overall Buckling.*—The critical buckling stress distributions $\sigma_y^{(+)}$ have been shown to possess the property of causing buckling of the leading (or trailing) edge simultaneously with overall buckling in torsion or flexure. These critical stress distributions may therefore be used as a criterion for deciding whether leading-edge buckling will occur before or after overall buckling in cases in which the actual stresses $\sigma_y$ differ from the stresses $\sigma_y^{(+)}$. For example, the solid wing of lenticular parabolic section treated in Section 3.2.1 is associated with a critical buckling stress

distribution which varies as a parabola ($\xi^2 - 1/5$), across the chord. If the actual stress distribution varies as a quartic ($\xi^4 - 3/35$), across the chord the stresses are more localised in the region of the leading and trailing edges, and localised buckling will occur there before overall buckling. Conversely, if the actual stress distribution varies in a V-shape ($|\xi| - 3/8$), across the chord, overall buckling will occur first. These qualitative statements can be confirmed in a quantitative manner by using later results of the present paper together with results from Refs. 3 or 4 from which the onset of overall buckling may be determined. Detailed calculations for the lenticular parabolic-section wing give

$$\frac{\text{Stress for localised buckling}}{\text{Stress for overall buckling}} = 0{\cdot}59, \text{ for the quartic stress variation}$$

$$= 1, \text{ for the parabolic stress variation}$$

$$= 1{\cdot}40, \text{ for the V-shaped stress variation.}$$

4. *Leading-Edge Buckling due to Aerodynamic-Heating Stresses.*—If the distribution of $\sigma_y$ stresses were identical to the $\sigma_y^{(+)}$ stress distribution it follows from equations (17) and (18) that leading-edge buckling would occur when

$$\sigma_{y,\,\text{edge}} = G\beta^2 \qquad (19)$$

for both solid and thin-walled wings. Now a comparison of the distributions of $\sigma_y^{(+)}$ in Figs. 3 and 4 with typical distributions of $\sigma_y$ due to aerodynamic heating shows one important difference: the stress distributions due to aerodynamic heating tend to be flatter over the mid-chord region and to rise more steeply towards the leading edge. From a consideration of average compressive stresses in the region of the leading edge it follows that equation (19) represents a lower limit for the true buckling stress. An upper limit for the buckling stress may be obtained by assuming that the buckling mode is given by equation (14) with $\lambda$ very small:

$$w = w_{\text{edge}} \operatorname*{Lim}_{\lambda \to 0} \sin(y/\lambda) \exp\{-(x + \tfrac{1}{2}c)/\lambda\}. \qquad (20)$$

Substituting equation (20) in equation (5) and integrating gives, for any $\sigma_y$ distribution:

$$\sigma_{y,\,\text{edge}} = G\beta^2 + 0(\lambda). \qquad (21)$$

As the wavelength $\lambda$ tends to zero this upper limit converges to the 'lower' limit given by equation (19). Equation (19) is therefore the criterion for determining the onset of leading-edge buckling, and the initial buckling mode is similar to that given by equation (20). The physical significance of this arises from the fact that this limiting mode produces a disturbance confined to a vanishingly narrow strip along the leading edge. During buckling under any distribution of forces, the work done by the forces and the strain energy of bending depend only on the magnitude of $\sigma_{y,\,\text{edge}}$ and the wing geometry at the leading edge.

This physical explanation of the onset of leading-edge buckling is amplified in Appendix III, where a number of exact large-deflection solutions are derived. It is shown there that the wavelength increases after initial buckling.

4.1. *Summary of Results Obtained for Initial Buckling.*—To summarise the position so far, it will be noted that for both solid and thin-walled wings with sharp leading and trailing edges:

(i) For any wing section there is one particular chordwise distribution of $\sigma_y$, namely $\sigma_y^{(+)}$ given by equation (17) or (18), for which torsional buckling, flexural buckling or leading-edge and trailing-edge buckling are equally likely;

(ii) Aerodynamic-heating stresses generally rise more steeply towards the leading edge than do the $\sigma_y^{(+)}$ stresses; when this is so, leading-edge buckling occurs when the spanwise stress at the leading edge equals $G\beta^2$, and it occurs before overall buckling;

(iii) At the onset of leading edge buckling the spanwise wavelength is very small.

5. *Post-Buckling Behaviour.*—The variation of the wavelength and the magnitude of the buckles after initial buckling can be investigated only by using large-deflection theory. However, because of the inherent complexity of large-deflection theory it is possible to obtain exact solutions only for a limited range of $\sigma_y$ distributions.

It is shown in Appendix III that an exact large-deflection solution exists for a wing of arbitrary section if the $\sigma_y$ stresses that would exist if the wing were restrained from buckling, are of the form

$$\sigma_y = \sigma_y^{(+)} + \sigma_1 \exp\{-\psi(x + \tfrac{1}{2}c)\} + A_0 + A_1 x, \qquad (22)$$

where $A_0$ and $A_1$ are chosen to satisfy the conditions of self-equilibration, *i.e.*, equation (1). The parameters $\sigma_1$ and $\psi$ are arbitrary. If the stresses $\sigma_y$ are caused entirely by temperature effects it follows that exact solutions are possible whenever the chordwise temperature distribution is of the form

$$T(x) = T^{(+)} + T_1 \exp\{-\psi(x + \tfrac{1}{2}c)\} + B_0 + B_1 x, \qquad (23)$$

where $T^{(+)}$ is such as to produce stresses $\sigma_y^{(+)}$ and $T_1$, $\psi$, $B_0$ and $B_1$ are arbitrary.

During buckling the $\sigma_y$ stresses are reduced to $\sigma_y^{(+)}$ while the stresses $\sigma_x$ and $\tau_{xy}$ remain zero; the wing assumes the buckled form:

$$w = w_{\text{edge}} \sin(\tfrac{1}{2}\psi y) \exp\{-\tfrac{1}{2}\psi(x + \tfrac{1}{2}c)\}, \qquad (24)$$

where

$$\left.\begin{aligned} w_{\text{edge}} &= \frac{4}{\psi}\left(\frac{\sigma_1}{E}\right)^{1/2} \\ &= \frac{4}{\psi}(\alpha T_1)^{1/2} \end{aligned}\right\} \qquad (25)$$

5.1. *Approximate Post-Buckling Solutions.*—It will generally be the case that the $\sigma_y$ stresses cannot be represented exactly by equation (22) and approximate methods of calculation are then necessary. It has already been shown that the onset of leading-edge buckling depends only on the stress at the leading edge, and from similar physical considerations it is to be expected that the buckled form depends primarily on the stress at the leading edge and on the average rate of change of stress in the region of the leading edge. By equating the actual values of $\sigma_{y,\,\text{edge}}$ and $(d\sigma_y/dx)_{\text{edge}}$, say, with the corresponding values obtained from equation (22), it is possible to determine values for $\sigma_1$ and $\psi$, and hence an approximate buckled form from equations (24) and (25). Thus

$$\left.\begin{aligned} \sigma_{y,\,\text{edge}} &= G\beta^2 + \sigma_1 + A_0 - \tfrac{1}{2}cA_1 \\ \left(\frac{d\sigma_y}{dx}\right)_{\text{edge}} &= \frac{5}{2}G\beta\left(\frac{d\beta}{dx}\right)_{\text{edge}} - \psi\sigma_1 + A_1 \end{aligned}\right\}, \qquad (26)$$

where, for a symmetrical wing section,

$$\left.\begin{aligned} A_0 &= \frac{-\sigma_1 \int_{-c/2}^{c/2} \bar{t} \exp\{-\psi(x+\tfrac{1}{2}c)\}\,dx}{\int_{-c/2}^{c/2} \bar{t}\,dx} \\ A_1 &= \frac{-\sigma_1 \int_{-c/2}^{c/2} x\bar{t} \exp\{-\psi(x+\tfrac{1}{2}c)\}\,dx}{\int_{-c/2}^{c/2} x^2\bar{t}\,dx} \end{aligned}\right\} \quad \ldots \quad (27)$$

In many instances the value of $\psi$ will be sufficiently large for the constants $A_0$ and $A_1$ to be neglected. The parameters $\sigma_1$ and $\psi$ are then given simply by:

$$\left.\begin{aligned} \sigma_1 &\simeq \sigma_{y,\,\text{edge}} - G\beta^2 \\ \psi &\simeq \frac{\frac{5}{2}G\beta\left(\frac{d\beta}{dx}\right)_{\text{edge}} - \left(\frac{d\sigma_y}{dx}\right)_{\text{edge}}}{\sigma_1} \end{aligned}\right\} \quad \ldots \quad (28)$$

6. *Examples.*—The purpose of these examples is to draw attention to the order of magnitude of leading-edge buckling. In the first example the reductions in the torsional and flexural rigidities at the onset of leading-edge buckling are determined and shown to be comparatively small.

(i) A 3 per cent solid steel wing of diamond section, for which

$$c = 20 \text{ in.}$$

$$\nu = 0{\cdot}25$$

$$\alpha = 1{\cdot}2 \times 10^{-5}/\text{deg C},$$

is subjected to a temperature distribution that varies parabolically across the chord. At what temperature difference will leading-edge buckling occur and how will the buckles vary with increasing temperature difference ?

The temperature distribution is given by

$$T = T_0 + (T_{\text{edge}} - T_0)\xi^2,$$

so that from equation (1) the stress distribution (away from tip effects) is given by

$$\sigma_y = E\alpha(T_{\text{edge}} - T_0)(\xi^2 - \tfrac{1}{6}). \quad \ldots \quad (29)$$

Thus

$$\begin{aligned} \sigma_{\text{edge}} &= \tfrac{5}{6} E\alpha(T_{\text{edge}} - T_0) \\ &= G\beta^2 \text{ at the onset of buckling} \\ &= \frac{E}{2(1+\nu)}\{0{\cdot}06\}^2 \text{ in this example.} \quad \ldots \quad (30) \end{aligned}$$

It follows from equation (30) that leading-edge buckling will occur when

$$T_{\text{edge}} - T_0 = \frac{6\{0{\cdot}06\}^2}{10(1+\nu)\alpha}$$

$$= 144 \text{ deg C.} \quad .. \quad .. \quad .. \quad .. \quad .. \quad .. \quad (31)$$

At this temperature difference it can be shown that the torsional and flexural rigidities have dropped to 0·72 and 0·83 respectively of their original (unheated) values. Note, too, that this temperature difference is independent of Young's modulus.

The mode after buckling may be determined approximately from equations (24), (25) and (28). From equation (28):

$$\sigma_1 \simeq \tfrac{5}{6} E\alpha\{(T_{\text{edge}} - T_0) - 144\} \quad .. \quad .. \quad .. \quad (32)$$

and

$$\psi \simeq \frac{4E\alpha}{c\sigma_1}(T_{\text{edge}} - T_0) \quad .. \quad .. \quad .. \quad .. \quad .. \quad (33)$$

since, for a diamond section $d\beta/dx$ is zero.

Equation (25) now gives

$$w_{\text{edge}} \simeq 0{\cdot}76c\left\{(T_{\text{edge}} - T_0) - 144\right\}\left(\frac{\alpha}{T_{\text{edge}} - T_0}\right)^{1/2}, \quad .. \quad .. \quad (34)$$

and when

$$T_{\text{edge}} - T_0 = 169 \text{ deg C} \quad \text{or} \quad 194 \text{ deg C}, \quad \text{say,}$$

$$w_{\text{edge}} \simeq 0{\cdot}10 \text{ in.} \quad \text{or} \quad 0{\cdot}19 \text{ in.}$$

and the spanwise buckle wavelength $= 2\pi/\psi$

$$= 3{\cdot}9 \text{ in.} \quad \text{or} \quad 6{\cdot}8 \text{ in.}$$

These numerical results are typical of the post-buckling behaviour of the leading edge in that they show that immediately after initial buckling the wavelength and the magnitude of the buckles increase linearly with the temperature of the leading edge.

(ii) It is required to obtain a value for $\beta$ such that leading-edge buckling will not occur under certain flight conditions. We shall confine attention to flight in the stratosphere where

$$T_{\text{air}} \simeq 210 \text{ deg } K$$

and the recovery temperature for laminar flow is given by

$$T_{\text{r}} \simeq 210(1 + 0{\cdot}17M^2). \quad .. \quad .. \quad .. \quad .. \quad .. \quad (35)$$

If the wing is originally at a temperature corresponding to steady state conditions at $M_1$ a rapid acceleration to $M_2$ will cause a leading-edge temperature given by equation (35). This is because the heat transfer is so high at the leading edge that there is virtually no time delay. Further, for a short acceleration time, the main body of the wing will be virtually unstressed and the compressive stress

at the leading edge will be given approximately by

$$\sigma_{\text{edge}} \doteq 210 \times 0{\cdot}17 \times E\alpha\,(M_2^2 - M_1^2). \quad .. \quad .. \quad .. \quad (36)$$

If expression (36) is equated to $G\beta^2$, it is found that

$$\beta \doteq 9{\cdot}4\alpha^{1/2}(M_2^2 - M_1^2)^{1/2}. \quad .. \quad .. \quad .. \quad .. \quad (37)$$

For a steel in which $\alpha = 1{\cdot}2 \times 10^{-5}$/deg C:

$$\beta \doteq 0{\cdot}032(M_2^2 - M_1^2)^{1/2},$$

while for a Duralumin in which $\alpha = 2{\cdot}3 \times 10^{-5}$/deg C:

$$\beta \doteq 0{\cdot}045(M_2^2 - M_1^2)^{1/2}.$$

These approximate results show that if leading-edge buckling is to be avoided the angle $\beta$ must exceed a critical angle which is proportional to a simple function of the Mach numbers at start and finish of a rapid acceleration.

7. *Conclusions.*—This paper has considered the occurrence of leading-edge buckling in wings which may be regarded structurally as plates of variable rigidity. An inverse method of solution has been used in which a 'critical buckling stress distribution' appropriate to a given wing section is investigated. This critical buckling stress distribution has the unique property that buckling in any one of an infinite variety of modes (including torsion, flexure and leading-edge waving) is then equally probable. Comparisons with the stress distributions caused by aerodynamic heating shows that leading-edge buckling will occur when the spanwise stress at the leading edge exceeds (the shear modulus of the material) $\times$ (the angle at the leading edge formed by tangents to the top and bottom surfaces)$^2$, and the spanwise wavelength of the buckles is initially very small. The post-buckling behaviour of the mode has been investigated using large-deflection theory.

## LIST OF SYMBOLS (See Fig. 1)

| | | |
|---|---|---|
| $c$ | | Wing chord |
| $t$ | | Wing thickness |
| $0x$, $0y$ | | Cartesian axes, $0y$ measured spanwise, $0x$ measured chordwise from the mid-chord of the wing |
| $t_0$ | | Wing thickness at mid-chord |
| $h$ | | Skin thickness in thin-walled wing |
| $\bar{t}$ | | Thickness of direct stress bearing material |
| | $=$ | $t$ for solid wing |
| | $=$ | $2h$ for thin-walled wing |
| $E$, $G$ | | Young's modulus, shear modulus (assumed constant) |
| $\nu$ | | Poisson's ratio |
| $D$ | $=$ | $Et^3/\{12(1-\nu^2)\}$ for solid wing |
| | $=$ | $Eht^2/\{2(1-\nu^2)\}$ for thin-walled wing |
| $\alpha$ | | Coefficient of thermal expansion (assumed constant) |
| $\beta$ | | Angle at leading edge formed by lines which are normal to the leading edge and tangents to top and bottom surfaces |
| $w$ | | Deflection normal to plane of wing |
| $\sigma_x$, $\sigma_y$, $\tau_{xy}$ | | Direct and shear stresses in plane of wing ($\sigma_x$ and $\sigma_y$ positive if compressive) |
| $N_y$ | | Spanwise middle-surface forces/unit length due to temperature effects (positive if compressive) |
| $\Phi$, $\Phi_0$ | | Force functions defined by equations (2), (3) and (4) |
| $\varkappa_1$, $\varkappa_2$ | | Principal curvatures |
| $T$ | | Average temperature through wing thickness |
| $M$ | | Mach number |
| $\xi$ | $=$ | $2x/c$ |
| $\gamma$, $\lambda$, $\psi$ | | Parameters |
| $\sigma_1$, $T_1$<br>$A_0$, $A_1$, $B_0$, $B_1$ | | Arbitrary constants |

Indices $^{(+)}$ and $^{(-)}$ refer to 'positive' and 'negative' critical stress distributions

$\iint \ldots dx\, dy$ $=$ Integral over complete wing

*Additional Symbols Used Only in the Appendices*

| | |
|---|---|
| $I$ | Integral defined by equation (38) |
| $u$, $v$ | Displacements in plane of wing referred to unbuckled state |
| $\Delta\varepsilon_x$, $\Delta\varepsilon_y$, $\Delta\gamma_{xy}$ | Changes in strains from unbuckled state |
| $\Delta\sigma_x$, $\Delta\sigma_y$, $\Delta\tau_{xy}$ | Changes in stresses from unbuckled state |
| $\bar{\sigma}_y$ | Stress in unbuckled state ($\bar{\sigma}_x$ and $\bar{\tau}_{xy}$ being zero) |
| $f$ | Displacement function introduced in equation (55) |
| $A, \Lambda$ | Introduced in equation (58) |

---

## LIST OF REFERENCES


| *No.* | *Author* | *Title, etc.* |
|---|---|---|
| 1 | J. Kaye ... ... ... ... ... | The transient temperature distributions in a wing flying at supersonic speeds. *J. Ae. Sci.* December, 1950. |
| 2 | H. L. Dryden and J. E. Duberg ... ... | Aero-elastic effects of aerodynamic heating. Paper presented to 5th General Assembly, A.G.A.R.D., Ottawa, Canada. June, 1955. |
| 3 | E. H. Mansfield ... ... ... ... | The influence of aerodynamic heating on the flexural rigidity of a thin wing. R. & M. 3115. September, 1957. |
| 4 | S. L. Kochanski and J. H. Argyris ... | Some effects of kinetic heating on the stiffness of thin wings. Parts I and II. *Aircraft Engineering*. October, 1957 and February, 1958. |
| 5 | S. Timoshenko ... ... ... ... | Theory of Elastic Stability. McGraw-Hill. 1936. |
| 6 | E. H. Mansfield ... ... ... ... | Combined flexure and torsion of a class of heated thin wings. R. & M. 3195. March, 1958. |


---

## APPENDIX I

*Transformation of an Integral*

It is shown here how the integral $I$ may be transformed, where

$$I \equiv \int_0^\infty \int_{-c/2}^{c/2} \frac{d^2\Phi_0}{dx^2} \left(\frac{\partial w}{\partial y}\right)^2 dx\, dy \qquad (38)$$

and $\Phi_0$ (written hereafter for convenience as $\Phi$) is a function of $x$ that satisfies the boundary conditions

$$[\Phi]_{x=\pm c/2} = \left[\frac{d\Phi}{dx}\right]_{x=\pm c/2} = 0. \qquad (39)$$

Integrating $I$ by parts and using equation (39) gives

$$\begin{aligned}
I &= \int_0^\infty dy \left\{ \left| \frac{d\Phi}{dx} \left(\frac{\partial w}{\partial y}\right)^2 \right|_{-c/2}^{c/2} - 2\int_{-c/2}^{c/2} \frac{d\Phi}{dx} \frac{\partial w}{\partial y} \frac{\partial^2 w}{\partial x\, \partial y}\, dx \right\} \\
&= -2\int_0^\infty dy \int_{-c/2}^{c/2} \frac{\partial w}{\partial y} \frac{\partial^2 w}{\partial x\, \partial y}\, d\Phi \\
&= -2\int_0^\infty dy \left\{ \left| \Phi \frac{\partial w}{\partial y} \frac{\partial^2 w}{\partial x\, \partial y} \right|_{-c/2}^{c/2} - \int_{-c/2}^{c/2} \Phi \frac{\partial}{\partial x} \left( \frac{\partial w}{\partial y} \frac{\partial^2 w}{\partial x\, \partial y} \right) dx \right\} \\
&= 2\int_0^\infty \int_{-c/2}^{c/2} \Phi \left\{ \left( \frac{\partial^2 w}{\partial x\, \partial y} \right)^2 + \frac{\partial w}{\partial y} \frac{\partial^3 w}{\partial x^2\, \partial y} \right\} dx\, dy \\
&= 2\int_0^\infty \int_{-c/2}^{c/2} \Phi \left( \frac{\partial^2 w}{\partial x\, \partial y} \right)^2 dx\, dy + 2\int_{-c/2}^{c/2} dx \int_0^\infty \Phi \frac{\partial w}{\partial y}\, d\left( \frac{\partial^2 w}{\partial x^2} \right) \\
&= 2\int_0^\infty \int_{-c/2}^{c/2} \Phi \left( \frac{\partial^2 w}{\partial x\, \partial y} \right)^2 dx\, dy \\
&\quad + 2\int_{-c/2}^{c/2} dx \left\{ \left| \Phi \frac{\partial w}{\partial y} \frac{\partial^2 w}{\partial x^2} \right|_0^\infty - \int_0^\infty \frac{\partial^2 w}{\partial x^2} \frac{\partial}{\partial y} \left( \Phi \frac{\partial w}{\partial y} \right) dy \right\} \\
&= 2\int_0^\infty dy \int_{-c/2}^{c/2} \Phi \left\{ \left( \frac{\partial^2 w}{\partial x\, \partial y} \right)^2 - \frac{\partial^2 w}{\partial x^2} \frac{\partial^2 w}{\partial y^2} \right\} dx \qquad (40)
\end{aligned}$$

provided the term $\left| \Phi \frac{\partial w}{\partial y} \frac{\partial^2 w}{\partial x^2} \right|_0^\infty$ is zero, or finite compared with the other infinitely large terms, which is so, for example, if $w$ is periodic in $y$.

## APPENDIX II

### *Buckling Characteristics of the Force Function $\Phi = \gamma D$ ($\gamma$ negative)*

If the denominator of equation (11) is positive we may write

$$\gamma = 1 - \nu - \frac{\iint \left\{ D(\varkappa_1 + \varkappa_2)^2 \right\} dx\, dy}{2 \iint \left\{ D(\varkappa_1 + \varkappa_2)^2 \right\} \left( \frac{\varkappa_1 \varkappa_2}{(\varkappa_1 + \varkappa_2)^2} \right) dx\, dy} \quad .. \quad .. \quad (41)$$

and because the terms in braces above are equal and everywhere positive the minimum (negative) value for $\gamma$ occurs when

$$\frac{\varkappa_1 \varkappa_2}{(\varkappa_1 + \varkappa_2)^2}$$

is a maximum, *i.e.*, when

$$\varkappa_1 - \varkappa_2 = 0. \quad .. \quad .. \quad .. \quad .. \quad .. \quad .. \quad (42)$$

Substituting equation (42) in (41) gives

$$\left.\begin{aligned} \gamma^{(-)} &= -(1 + \nu) \\ \Phi^{(-)} &= -(1 + \nu) D \end{aligned}\right\} \quad .. \quad .. \quad .. \quad .. \quad (43)$$

so that

The buckling mode of deformation represented by equation (42) may be expressed in terms of $w(x, y)$ by using equations (10). Thus

$$\begin{aligned} (\varkappa_1 - \varkappa_2)^2 &\equiv (\varkappa_1 + \varkappa_2)^2 - 4\varkappa_1 \varkappa_2 \\ &\equiv (\nabla^2 w)^2 - 4 \left\{ \frac{\partial^2 w}{\partial x^2} \frac{\partial^2 w}{\partial y^2} - \left( \frac{\partial^2 w}{\partial x\, \partial y} \right)^2 \right\} \\ &\equiv \left[ \frac{\partial^2 w}{\partial x^2} - \frac{\partial^2 w}{\partial y^2} \right]^2 + 4 \left[ \frac{\partial^2 w}{\partial x\, \partial y} \right]^2 \quad .. \quad .. \quad .. \quad .. \quad (44) \end{aligned}$$

and by virtue of equation (42) each of the terms above in square brackets vanishes so that, apart from rigid body terms,

$$w \propto x^2 + y^2. \quad .. \quad .. \quad .. \quad .. \quad .. \quad (45)$$

---

## APPENDIX III

### *Large Deflection Solutions*

Consider first the condition of compatibility. It is convenient to measure the displacements $u$, $v$, $w$ with reference to the unbuckled and unstable state. In the buckled state the changes in strains $\Delta\varepsilon_y$, etc., are then given by

$$\left.\begin{aligned} \Delta\varepsilon_y &= \frac{\partial v}{\partial y} + \frac{1}{2}\left(\frac{\partial w}{\partial y}\right)^2 \\ \Delta\varepsilon_x &= \frac{\partial u}{\partial x} + \frac{1}{2}\left(\frac{\partial w}{\partial x}\right)^2 \\ \Delta\gamma_{xy} &= \frac{\partial u}{\partial y} + \frac{\partial v}{\partial x} + \frac{\partial w}{\partial x}\frac{\partial w}{\partial y} \end{aligned}\right\}. \qquad \ldots \quad (46)$$

The equation of compatibility is obtained by eliminating $u$, $v$ from equation (46) to give

$$\frac{\partial^2}{\partial x^2}\left(\Delta\varepsilon_y\right) + \frac{\partial^2}{\partial y^2}\left(\Delta\varepsilon_x\right) - \frac{\partial^2}{\partial x\,\partial y}\left(\Delta\gamma_{xy}\right) = \left(\frac{\partial^2 w}{\partial x\,\partial y}\right)^2 - \frac{\partial^2 w}{\partial x^2}\frac{\partial^2 w}{\partial y^2}. \qquad \ldots \quad (47)$$

The changes in strains are related to the changes in stresses $\Delta\sigma_y$, etc., by the equations

$$\left.\begin{aligned} -\Delta\varepsilon_y &= (\Delta\sigma_y - \nu\Delta\sigma_x)/E \\ -\Delta\varepsilon_x &= (\Delta\sigma_x - \nu\Delta\sigma_y)/E \\ \Delta\gamma_{xy} &= \Delta\tau_{xy}/G \end{aligned}\right\}, \qquad \ldots \quad (48)$$

where compressive stresses are regarded as positive.

Consider now the conditions of equilibrium. In the unbuckled state the only non-zero stresses are the $\bar{\sigma}_y$ stresses which are self-equilibrating; the changes in the middle-surface stresses therefore satisfy the equilibrium conditions:

$$\left.\begin{aligned} \frac{\partial}{\partial x}\left(\bar{t}\Delta\sigma_x\right) - \frac{\partial}{\partial y}\left(\bar{t}\Delta\tau_{xy}\right) &= 0 \\ \frac{\partial}{\partial y}\left(\bar{t}\Delta\sigma_y\right) - \frac{\partial}{\partial x}\left(\bar{t}\Delta\tau_{xy}\right) &= 0 \end{aligned}\right\}, \qquad \ldots \quad (49)$$

together with the overall conditions of self-equilibration:

$$\int \bar{t}\Delta\sigma_y\,dx = \int x\bar{t}\Delta\sigma_y\,dx = 0. \qquad \ldots \quad (50)$$

The equilibrium condition normal to the wing depends on the final stresses in the plate, i.e., on $\bar{\sigma}_y + \Delta\sigma_y$, $\Delta\sigma_x$, $\Delta\tau_{xy}$ since $\bar{\sigma}_x$, $\bar{\tau}_{xy}$ are zero. Because of the variable flexural rigidity the equilibrium equation involves derivatives of $D$:

$$DV^4w + 2\frac{\partial D}{\partial x}\left(\frac{\partial^3 w}{\partial x^3} + \frac{\partial^3 w}{\partial x\,\partial y^2}\right) + \frac{\partial^2 D}{\partial x^2}\left(\frac{\partial^2 w}{\partial x^2} + \nu\frac{\partial^2 w}{\partial y^2}\right) +$$

$$+ \bar{t}\left\{(\bar{\sigma}_y + \Delta\sigma_y)\frac{\partial^2 w}{\partial y^2} + \Delta\sigma_x\frac{\partial^2 w}{\partial x^2} - 2\Delta\tau_{xy}\frac{\partial^2 w}{\partial x\,\partial y}\right\} = 0. \qquad \ldots \quad (51)$$

In order to obtain solutions of equations (47) to (51) some restriction on the form of $\bar{\sigma}_y$ is necessary. It will now be shown that it is possible for $\Delta\sigma_x$ and $\Delta\tau_{xy}$ to be zero for some distributions of $\bar{\sigma}_y$, and the simplification resulting from this restriction enables a variety of solutions to be found.

Substituting

$$\Delta\sigma_x = \Delta\tau_{xy} = 0 \quad .. \quad .. \quad .. \quad .. \quad .. \quad .. \quad (52)$$

into equation (49) gives

$$\Delta\sigma_y = \text{function of } x\,, \quad .. \quad .. \quad .. \quad .. \quad .. \quad (53)$$

while from equations (47) and (48)

$$-\frac{\partial^2}{\partial x^2}(\Delta\sigma_y) = E\left\{\left(\frac{\partial^2 w}{\partial x\,\partial y}\right)^2 - \frac{\partial^2 w}{\partial x^2}\frac{\partial^2 w}{\partial y^2}\right\}. \quad .. \quad .. \quad .. \quad (54)$$

Now for leading-edge buckling we require the buckled mode to be of the form

$$w = f(x)\sin(y/\lambda) \quad .. \quad .. \quad .. \quad .. \quad .. \quad (55)$$

and equations (53) and (54) then give

$$\left(\frac{df}{dx}\right)^2 \cos^2(y/\lambda) + f\frac{d^2 f}{dx^2}\sin^2(y/\lambda) = \text{function of } x, \quad .. \quad .. \quad (56)$$

so that

$$\left(\frac{df}{dx}\right)^2 = f\frac{d^2 f}{dx^2} \quad .. \quad .. \quad .. \quad .. \quad .. \quad (57)$$

and $f$ is therefore of the form

$$= A\,e^{-x/\Lambda}, \quad .. \quad .. \quad .. \quad .. \quad .. \quad (58)$$

where $A$ and $\Lambda$ are arbitrary. An obvious choice for $\Lambda$ is to take

$$\Lambda = \lambda \quad .. \quad .. \quad .. \quad .. \quad .. \quad .. \quad (59)$$

as suggested by results obtained in the main body of the report.

Substituting

$$w = A\,e^{-x/\lambda}\sin(y/\lambda) \quad .. \quad .. \quad .. \quad .. \quad (60)$$

in equation (54) gives

$$-\frac{\partial^2}{\partial x^2}(\Delta\sigma_y) = EA^2\lambda^{-4}\,e^{-2x/\lambda}, \quad .. \quad .. \quad .. \quad .. \quad .. \quad (61)$$

whence

$$\Delta\sigma_y = -\tfrac{1}{4}EA^2\lambda^{-2}\,e^{-2x/\lambda} + \text{(linear terms to be chosen so as to satisfy equation (50))}. \quad .. \quad (62)$$

Similarly, substituting equation (60) in (51) gives

$$t(\bar{\sigma}_y + \Delta\sigma_y) = (1-\nu)\frac{\partial^2 D}{\partial x^2}, \quad .. \quad .. \quad .. \quad .. \quad .. \quad (63)$$

whence

$$\bar{\sigma}_y + \Delta\sigma_y = \sigma_y^{(+)} \quad .. \quad .. \quad .. \quad .. \quad .. \quad .. \quad (64)$$

from the definition of $\sigma_y^{(+)}$ given in equation (13) in the main body of the report. It follows that exact large deflection solutions for leading-edge buckling are possible whenever $\bar{\sigma}_y$ is of the form

$$\bar{\sigma}_y = \sigma_y^{(+)} + \tfrac{1}{4}EA^2\lambda^{-2}e^{-2x/\lambda} + \text{linear terms.} \quad .. \quad (65)$$

*Solutions for Overall Buckling.*—Exact solutions for buckling in torsion and flexure may be obtained from the above results by considering the limiting cases as $\lambda$ tends to infinity. It is, however more direct and simpler to substitute

$$\left.\begin{array}{l} w = Axy \\ \text{or} \quad \tfrac{1}{4}A(x^2 - y^2) \end{array}\right\} \quad .. \quad .. \quad .. \quad .. \quad .. \quad (66)$$

in equation (54) to obtain

$$-\frac{\partial^2}{\partial x^2}(\Delta\sigma_y) = EA^2, \quad .. \quad .. \quad .. \quad .. \quad .. \quad .. \quad (67)$$

from which it follows that

$$\bar{\sigma}_y = \sigma_y^{(+)} + \tfrac{1}{2}EA^2x^2 + \text{linear terms.} \quad .. \quad .. \quad (68)$$

By the same token we may obtain solutions for 'negative' overall buckling by substituting

$$w = \tfrac{1}{4}A(x^2 + y^2) \quad .. \quad .. \quad .. \quad .. \quad .. \quad (69)$$

in equation (54) to obtain

$$\frac{\partial^2}{\partial x^2}(\Delta\sigma_y) = EA^2, \quad .. \quad .. \quad .. \quad .. \quad .. \quad .. \quad (70)$$

from which it follows that

$$\bar{\sigma}_y = \sigma_y^{(-)} - \tfrac{1}{2}EA^2x^2 + \text{linear terms.} \quad .. \quad .. \quad (71)$$

Particular examples of equations (68) and (71) were discussed in Ref. 6.

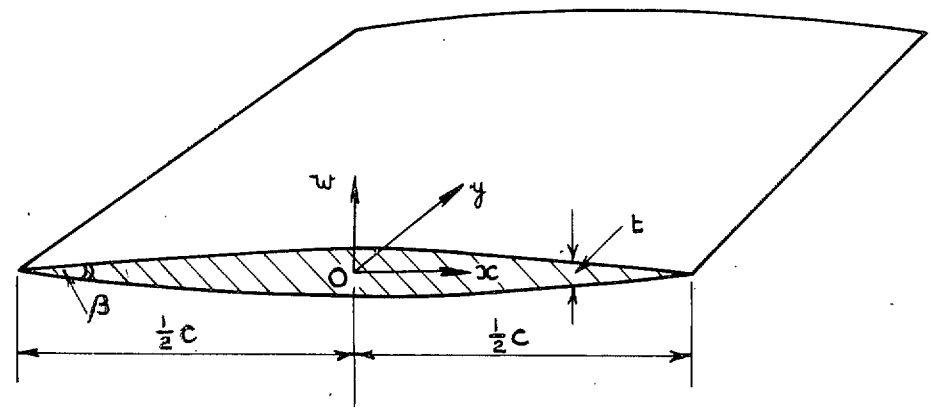


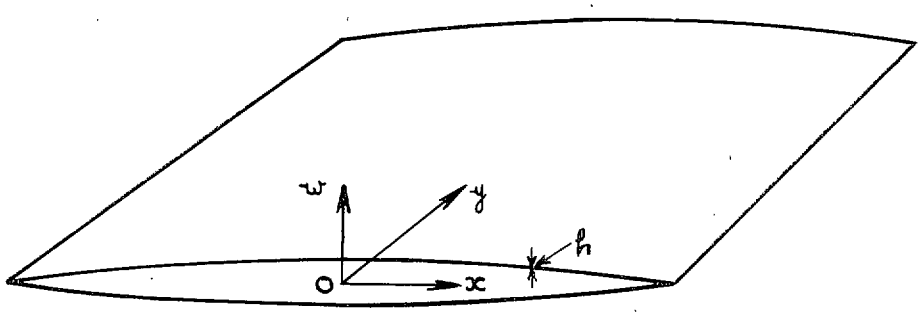


FIG. 1. Notation for solid and thin-walled wings.

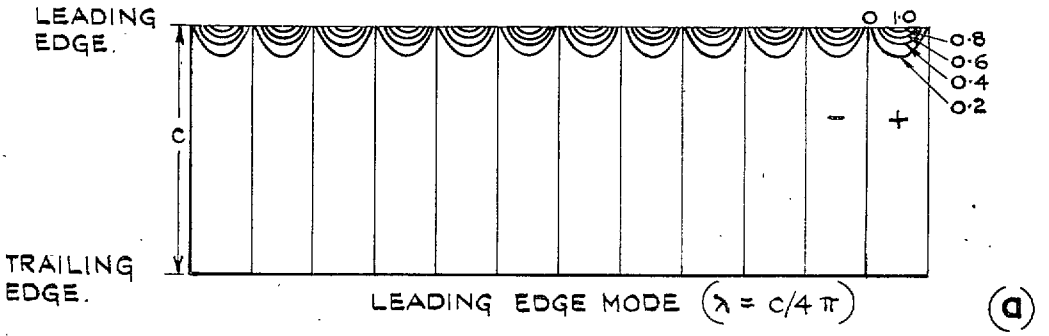


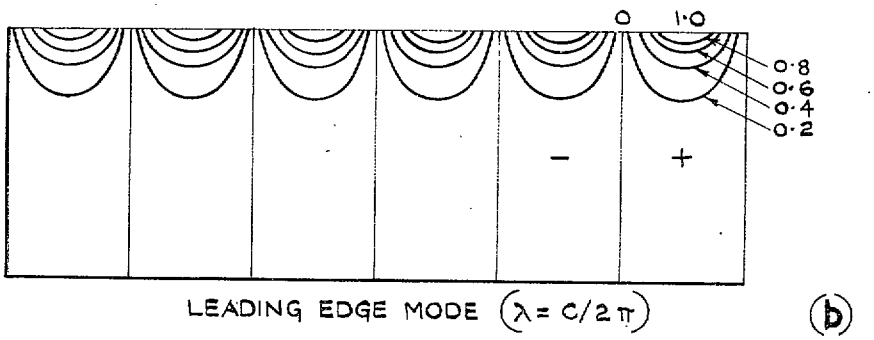


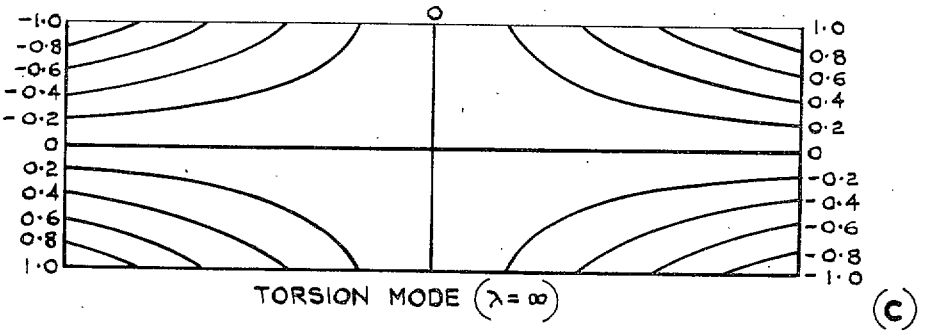


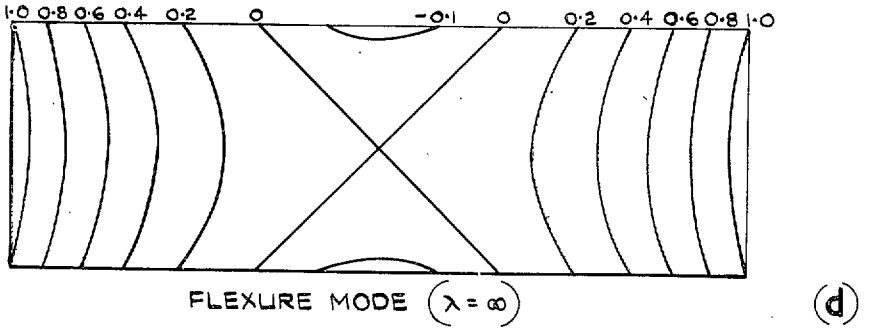


FIGS. 2a to 2d. Deflection contours for buckling modes given by equations (14), 15) and (16).

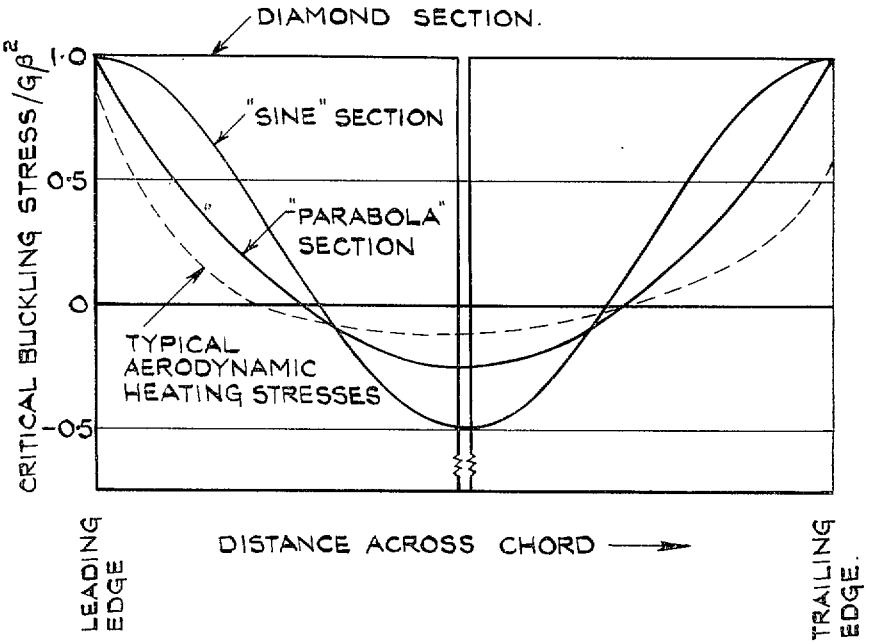


FIG. 3. Critical buckling stress distributions for solid wing sections.

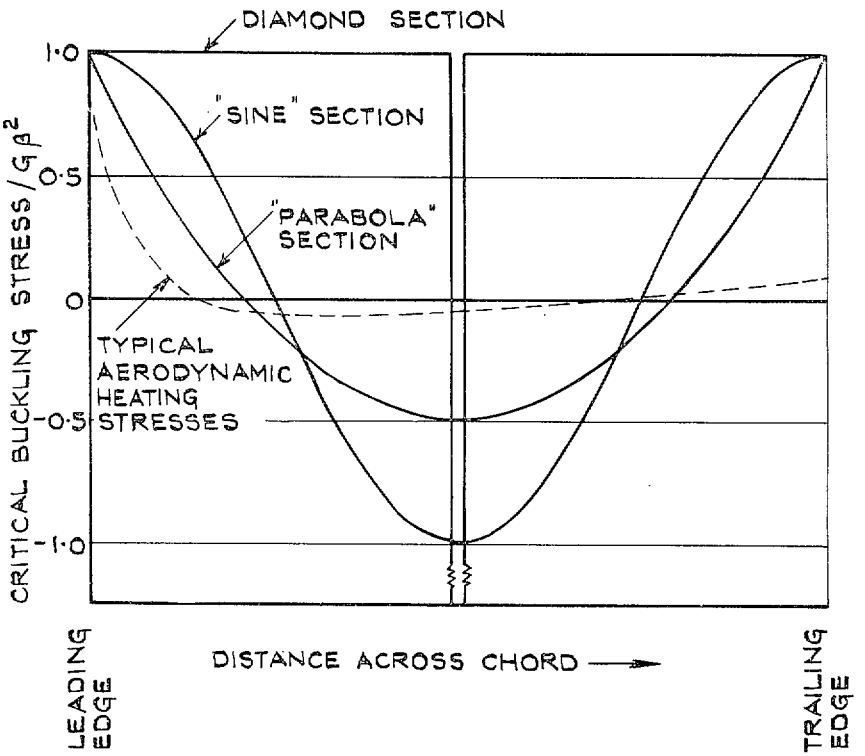


FIG. 4. Critical buckling stress distributions for thin-walled wing sections.



Printed in England under the authority of Her Majesty's Stationery Office by F. Mildner & Sons, London, E.C.1
(50618) Wt. 61 K5 10/60

Published by
HER MAJESTY'S STATIONERY OFFICE

To be purchased from
York House, Kingsway, London w.c.2
423 Oxford Street, London w.1
13A Castle Street, Edinburgh 2
109 St. Mary Street, Cardiff
39 King Street, Manchester 2
50 Fairfax Street, Bristol 1
2 Edmund Street, Birmingham 3
80 Chichester Street, Belfast 1
or through any bookseller

R. & M. No. 3197

S.O. Code No. 23-3197